This is a post-referee draft, the final version is available at

https://doi.org/10.1016/j.scriptamat.2019.12.019

High-Velocity Water Vapour Corrosion of Yb-Silicate: Sprayed vs. Sintered Body

Emine Bakan[a]*, Moritz Kindelmann[a], Willy Kunz[b], Hagen Klemm[b], Robert Vaßen[a]

[a]Forschungszentrum Jülich GmbH, Institute of Energy and Climate Research IEK-1, 52425 Jülich, Germany

[b]Fraunhofer Institute for Ceramic Technologies and Systems, IKTS Dresden, 01277 Dresden, Germany

*Corresponding Author. Forschungszentrum Jülich GmbH, Institute of Energy and Climate Research IEK-1, 52425 Jülich, Germany. Tel: +49 2461 61 2785; Fax: +49 2461 61 2455, e-mail: e.bakan@fz-juelich.de.

The water vapor corrosion of Yb-silicates is of interest to their application as environmental barrier coatings in gas turbine technology. In this study, densified samples from the Yb-silicate powder, as well as plasma-sprayed free-standing Yb-silicate coating were tested at a high-velocity steam rig (T=1400 °C, v=90 m/s, P_{H2O}=0.19 atm) for microstructural comparison. After the test, the measured weight losses of the coatings were larger than that of the densified sample. At the same time, the thicknesses of the corroded scales at the coating surfaces were found to be thicker than that of the sintered sample by a factor of two.

Keywords: Environmental barrier coatings (EBC); plasma spray; FAST-SPS; CMC; SiC/SiC

SiC/SiC Ceramic Matrix Composites (CMCs) are advanced structural materials developed for gas turbine engines. They offer vastly improved temperature capability and lower weight with respect to Ni-based superalloy materials that are used in the high-temperature sections of the gas turbines. SiC forms a silica scale at high temperatures however that reacts with the water vapor and volatilizes in the combustion environment [1]. Environmental barrier coatings (EBC) are applied to the surface of these Si-based components in order to shield them from the water-vapor containing atmosphere of the engine. Several material compositions including mullite [2], barium-strontium-aluminosilicate (BSAS) [3] and rare-earth silicates (RES) [4] have been investigated as candidate EBC systems. Volatility resistance of RES was shown to be superior to BSAS and mullite, while RE mono-silicates (REMS) were reported to be chemically more stable than the RE di-silicates (REDS) [4]. Due to greater CTE of REMS, however, which induces higher stresses in the thermally cycled coatings and hence cracking, REDS, particularly $Y_2Si_2O_7$ and $Yb_2Si_2O_7$ are widely accepted as the best candidate materials.

The EBC degradation is not an extensively studied topic thus far primarily due to the requirement of advanced test rigs wherein engine like conditions (high temperature, high pressure, high-velocity gas flow, and high content of water vapor) can be simulated. Furthermore, the deposition of $Yb_2Si_2O_7$ EBCs demands sophisticated solutions because the manufacturing of a dense (crack and pore-free) EBC by conventional methods such as atmospheric plasma spraying is not possible due to high residual stresses generated in the layers. These stresses are mainly related to high Yb_2SiO_5 content in the $Yb_2Si_2O_7$ layers associated with the Si evaporation from the feedstock during spraying and secondly with the

high cooling rate of the molten particles on a cold substrate. As a result of these, fully amorphous and dense coatings but with periodic vertical cracking can be generated by the conventional atmospheric plasma spray (APS) method. These coatings become more porous and cracked as a result of post recrystallization when exposed to heat. For that reason, efforts have been made to solve these problems by increasing the substrate temperatures above 1000 °C or using different thermal spray methods that allow high-velocity deposition of partially molten particles [2, 5, 6]. Consequently, there are only a few studies investigating the environmental stability of coatings rather than densified powders which lacks the aforementioned characteristics of the coatings. Besides, even if the coatings are being tested, due to different deposition methods with high/low substrate temperatures, the coating characteristics vary significantly, as well. Considering that the test conditions (temperature, gas velocity etc.) of the rarely reported water vapor corrosion studies also differ, comparison of these results becomes quite difficult.

Richards et al. reported that after 2000 h steam cycling test (v=4.4 cm/s, T=1316 °C, 90% vol. H_2O /10% vol.O_2, 1 h high temperature exposure at each cycle) of a dense and crystalline $Yb_2Si_2O_7$ coating, a Yb_2SiO_5 layer with a thickness of about 15 µm grows at the surface via the following reaction pathway [7]:

$$2Yb_2Si_2O_7\ (s) + 2H_2O\ (g) \rightarrow Yb_2SiO_5\ (s) + Si(OH)_4\ (g) \quad (1)$$

As a result of high CTE mismatch stresses in Yb_2SiO_5 during the thermal cycling, vertical cracking was observed in this work within the growing Yb_2SiO_5 layer.

In a former study, the authors investigated the environmental stability of amorphous and crystalline $Yb_2Si_2O_7$-Yb_2SiO_5 mixed-phase APS coatings in a high-velocity steam rig (v=100 m/s, T=1200 °C, P_{H2O}=0.27 atm, t=200 h, 4 interruptions made during the test in order to allow weight measurements of the samples) [8]. Instead of a continuous Yb_2SiO_5 layer, a very porous (about 80 %) and 25 µm thick corroded layer, that was found to be rich in the Yb_2SiO_5 phase was observed at the surface of the amorphous layer while no morphological change was identified at the surface of the crystalline coating.

In this study, in order to understand the effect of crystallinity, phase composition and microstructure (e.g. porosity, grain size) on the water vapor corrosion kinetics at elevated temperatures, three different types of samples were prepared and tested at the same conditions. Using a $Yb_2Si_2O_7$ feedstock (Oerlikon Metco US Inc., Westbury, New York, USA), a 3 mm thick coating was deposited on a 50 x 50 x 5mm^3 stainless steel substrate. A MultiCoat system (Oerlikon Metco, Wohlen, Switzerland) with a three-cathode TriplexPro 210 spray torch mounted on a six-axis robot (IRB 2400, ABB, Switzerland) was employed for the APS experiment. After the deposition, the coating was removed from the substrate mechanically to obtain a free-standing coating which was subsequently cut into 3.0 x 3.8 x 36 mm^3 bars for testing. Some of these bars were heat-treated in air at 1500 °C for 40 h before testing. Another type of sample was prepared by FAST-SPS (Field Assisted Sintering Technique/ Spark Plasma Sintering) in an FCT H-HP-D25 facility (FCT Systeme GmbH, Rauenstein, Germany). In the sintering experiment, submicron powder size was used, which was obtained by ball milling the same $Yb_2Si_2O_7$ feedstock used for spray experiments for 24 h. The sintering was conducted using a heating rate of 100K/min, a sintering temperature of 1650°C, a dwell time of 5 minutes, a uniaxial pressure of 50MPa, and vacuum (~ 4 mbar) during the whole thermal cycle. A disk shape $Yb_2Si_2O_7$ sample with a diameter of 40 mm and thickness of 3 mm was manufactured by sintering and also cut into bars with the given dimensions above. All samples were tested in a high-velocity steam rig (v=90 m/s, T=1400 °C, P_{H2O}=0.19 atm, P=1 atm, t=200 h) and the details of the test set up are described elsewhere [8]. It should be noted that P_{H2O} was decreasing over time due to problems with the water evaporation unit during the test. The

test was interrupted after 25 h, 50 h, and 100 h in order to take weight measurements from the samples.

X-ray diffraction (XRD) of the as-sprayed coating (Fig.1) indicated that the material was almost fully amorphous after deposition. This is consistent with the knowledge from previous results that due to low deposition temperatures of the process (about 500 °C monitored via pyrometer) which remains below the crystallization temperature of the material (above 1000 °C), the molten particles deposited on the substrate cannot crystallize. After the heat treatment at 1500 °C, the coating was found to be crystalline and the peaks could be indexed with $Yb_2Si_2O_7$ (C2/m, JCPDS No 01-082-0734) and secondary monoclinic Yb_2SiO_5 (I2/a, JCPDS No 00-040-0386) phases. Similarly, the FAST-SPS sample was fully crystalline and was indexed with the same phases. Quantitative phase analysis (QPA) of the X-ray diffraction data of the coating after heat treatment and sintered body was performed using the Rietveld analysis method (TOPAS software, Bruker Corporation, Germany), and the samples were found to contain 30 wt.% and 8 wt.% Yb_2SiO_5, respectively. It should be noted that the feedstock used for the experiments had only ~3 wt.% Yb_2SiO_5 indicating significant Si-O evaporation during the plasma spraying process. Yb_2SiO_5 content increase in the sintered sample is possibly also due to the same phenomenon, however, because of the shorter processing time in the FAST-SPS as well as the relatively lower processing temperature in comparison with the plasma spraying, the influence is minor.

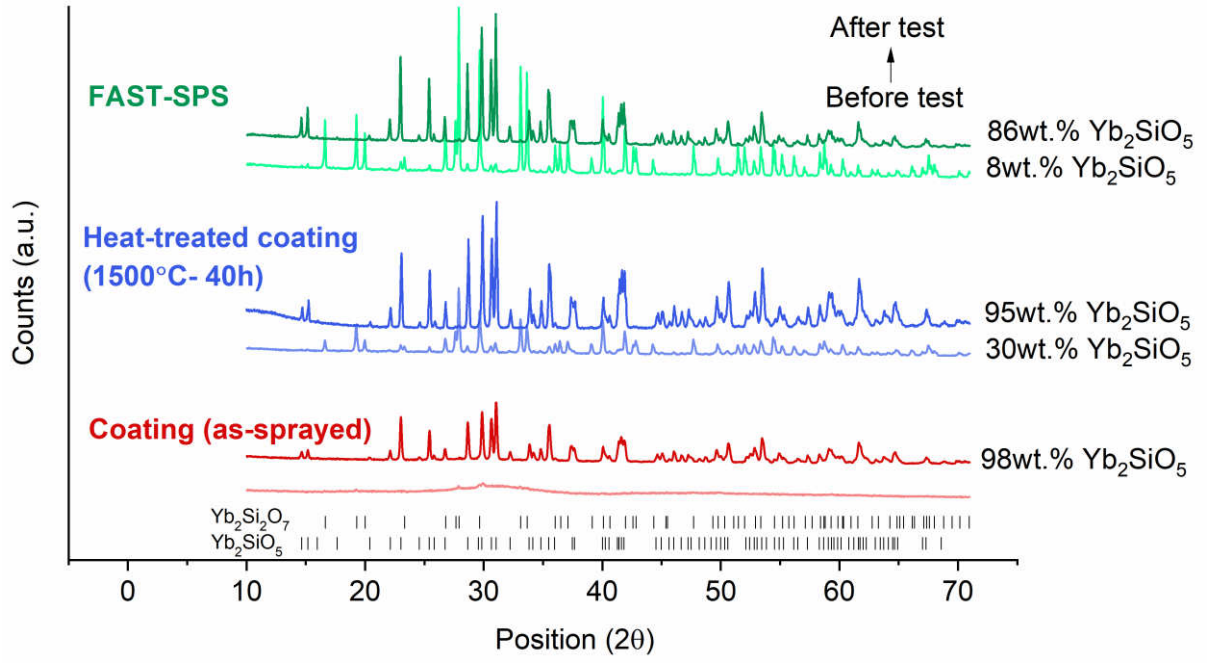

Figure 1: XRD diffractograms of as-sprayed coating, the same coating after heat treatment (1500 °C-40 h) and FAST-SPS sample before and after the test.

Fig.2 shows the recorded weight change of the Yb-silicate samples and SiC during corrosion testing. The results revealed parabolic corrosion kinetics for all samples. Given that linear weight loss kinetics were reported for SiC in the earlier studies conducted at this temperature [9], the observed parabolic weight loss in this study is presumably caused by a reducing water vapor pressure during the test. As the gas velocity and total pressure remained constant during the test, the weight loss is expected to reduce proportionally to the square of P_{H2O} assuming $Si(OH)_4$ as the main volatilization product. The parabolic weight loss in the Yb-silicate samples is affected by the reducing P_{H2O} level during the test, too, however, it is also known from a previous study [10] that under similar and constant test conditions the weight reduction in $Yb_2Si_2O_7$ as a function of time is also parabolic. Due to this parabolic dependence, the volatilization of $Yb_2Si_2O_7$ with the water vapor reaction is expected to be a diffusion-limited

process with inward diffusion of H_2O (g) or outward diffusion of $Si(OH)_4$ (g) being the rate-limiting step. The comparison of the weight losses between the coatings and the sintered powder sample revealed that the coatings have higher cumulative weight losses than the sintered powder sample at all times during 200 h (Fig.2). At the same time, the weight loss in the as-sprayed Yb-silicate coating was measured to be higher than that of the heat-treated coating sample.

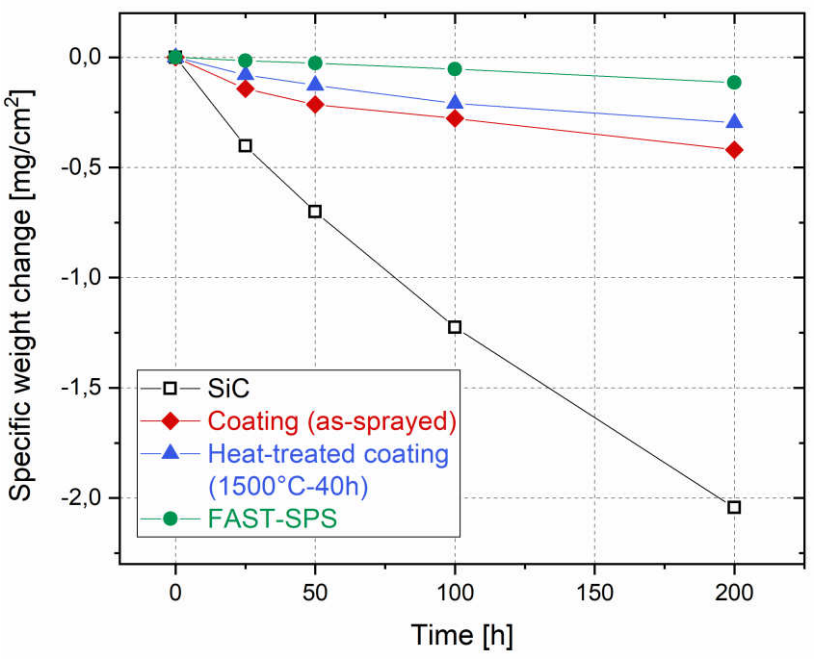

Figure 2: The recorded weight changes in the Yb-silicate and SiC samples during 200 h testing in water vapor containing atmosphere (P_{H2O}=0.19 atm) at 1400 °C, with a gas velocity of 90 m/s.

Figure 3 shows the microstructure of the Yb-silicate samples before and after testing. The porosity levels in the as-sprayed and heat-treated coatings before the test were determined using image analysis to be 3 and 7%, respectively (Fig.3a-b). The increase in the porosity content was attributed to crystallization shrinkage after the heat treatment. The porosity in the FAST-SPS sample was found to be less than 2% with the size of pores smaller than 1µm (Fig.3c). In contrast to that, the maximum pore sizes of 10-20 µm were detected in the as-sprayed and heat-treated coatings. Additionally, the average grain size (4-6 µm) in the FAST-SPS sample was observed to be larger than that of the crystalline coating (1-2 µm).

After the test, as a result of the water vapor reaction, a porous and microcracked Yb_2SiO_5 layer at the surface of each sample type was observed (Fig.3d-f). Assuming that $Si(OH)_4$ is the only volatile product of the $Yb_2Si_2O_7$ – Yb_2SiO_5 transformation and considering the theoretical densities of these two silicates (5.58 – 6.80 g/cm^3, respectively) a volume reduction of 26% is expected due to the transformation. No vertical cracking was observed in the Yb_2SiO_5 layers as reported by Richards et. al [7], probably due to fewer thermal cycles in this study and shorter testing time. A comparison of the microstructures of Yb_2SiO_5 layer formed at the surface of the $Yb_2Si_2O_7$ coatings and the sintered powder sample revealed significant differences in the pore morphology. Very large and spherical pores (> 5 µm) were observed in the Yb_2SiO_5 layer of the as-sprayed coating after testing in contrast to the heat-treated coating. In the heat-treated coating, the shape of the pores was found to be highly irregular and some large pores (~ 5 µm) were also noticed here in the Yb_2SiO_5 layer. In the FAST-SPS sample, small and spherical pores (<2 µm) similar to pores in the before test microstructure as well as larger pores that are elongated through the thickness of the Yb_2SiO_5 layer were recognized. These microstructural differences in the growing Yb_2SiO_5 layers are seemingly critical for the corrosion kinetics. Because the effective diffusion coefficient in the porous

Yb_2SiO_5 layer for the inward diffusion of water vapor and outward diffusion of $Si(OH)_4$ is controlled by the porosity, pore size, and shape as well as the pore connections (open or closed porosity).

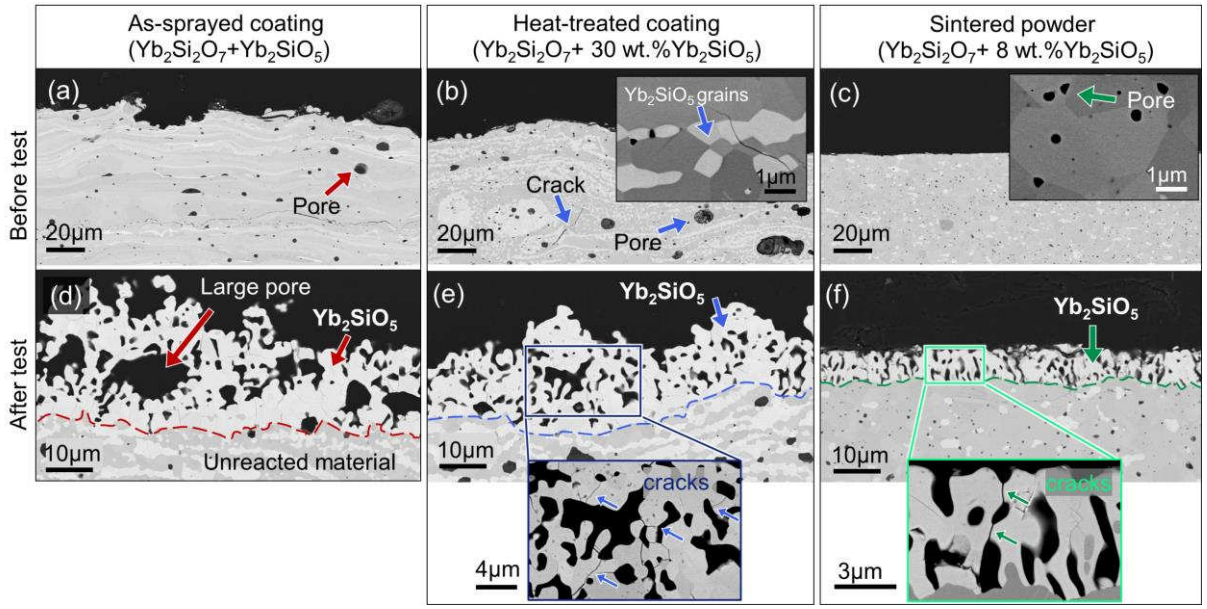

Figure 3: The microstructures of the Yb-silicate samples before (a-c) and after the test (d-f).

The comparison of the average thickness of the Yb_2SiO_5 layers formed on the different $Yb_2Si_2O_7$ samples is shown in Figure 4. The thickest Yb_2SiO_5 layer was measured at the surface of the as-sprayed coating, secondly in the heat-treated coating and at last in the FAST-SPS sample. This order is consistent with the measured weight losses of the same samples shown above in Fig. 2. Evidently, the corrosion kinetics of the $Yb_2Si_2O_7$ coatings is faster than that of the sintered $Yb_2Si_2O_7$ body. This is possibly associated with the higher volume of porosity in the coatings than that of the sintered sample. It might be that the pore network both in the Yb_2SiO_5 layer and in the unreacted material is also better connected in the coatings in comparison with the sintered sample, however further analyses are required to draw conclusions on that. Furthermore, the larger grain size distribution in the sintered body might have an influence on reduced corrosion rates, as the disordered structures at the grain boundaries are expected to have a lower resistance against water vapor attack. It is also important to note that, faster corrosion kinetics in the coatings was observed regardless of their higher Yb_2SiO_5 content (30 wt.%) compared to the sintered body (8 wt.%). This result implies the significant influence of microstructure on the corrosion kinetics as the Yb_2SiO_5 is the thermodynamically more stable phase and yet the coatings with higher Yb_2SiO_5 content show faster corrosion rates. The higher weight loss and at the same time the larger thickness of the formed Yb_2SiO_5 layer in the as-sprayed coating than that of the heat-treated, crystalline coating also suggest more pronounced corrosion in the former. The reason for that could be related to the large spherical pores in the Yb_2SiO_5 layer of the as-sprayed coating that are likely forming due to recrystallization of this coating during the initial stages of the testing. These pores could be facilitating the inward and outward diffusion of the gaseous reactant and reaction product by reducing the diffusion length and hence accelerating the corrosion.

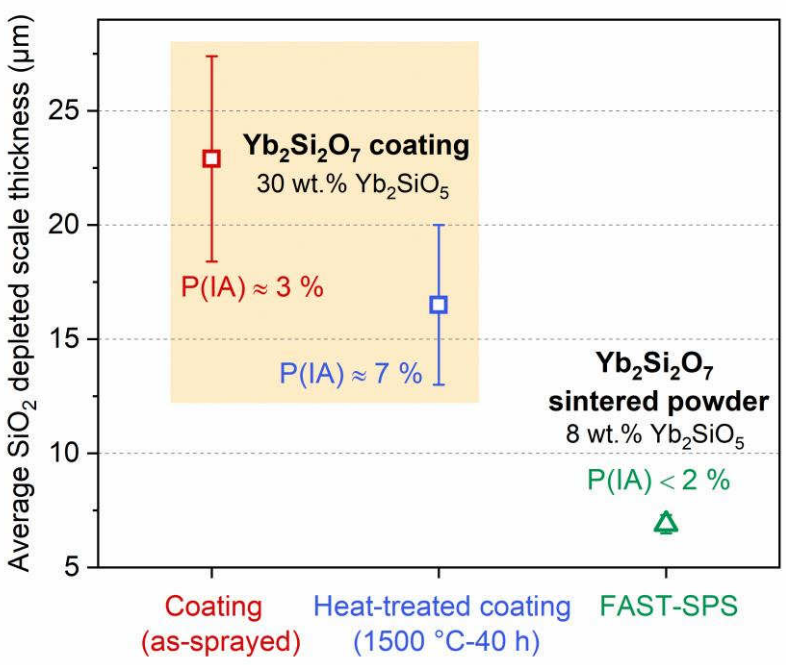

Figure 4: Average thickness of silica depleted scale (Yb_2SiO_5) at the surface of $Yb_2Si_2O_7$ coatings and sintered powder sample after the test (T=1400 °C, v=90 m/s, t=200 h). P(IA) indicates porosity of the samples determined by image analysis.

The Yb_2SiO_5 formation at the surface of the amorphous coating in this study, differently than the former work which was performed at 1200 °C, also indicates that the crystallization kinetics are faster at 1400 °C and can compete with the corrosion kinetics. Because at 1200 °C after 200 h, no continuous Yb_2SiO_5 layer but an 80% porous, 25 µm thick corroded layer was found in the former work at the surface of the amorphous coating [8]. Therefore for an amorphous microstructure, corrosion kinetics seems to be faster at the lower temperature due to hindered crystallization kinetics.

To summarize, the data presented in this work revealed that the kinetics of the water vapor reaction of $Yb_2Si_2O_7$ significantly depends on the microstructure. The thicknesses of the Yb_2SiO_5 scales that were formed at the surface of the sprayed $Yb_2Si_2O_7$ was at least double of that of the FAST-SPS sample under the same test conditions. This result is substantially important particularly when the high Yb_2SiO_5 content of the coatings in comparison with the FAST-SPS sample taken into account. Based on these findings, the more favorable microstructural features of the FAST-SPS sample such as small pore size and large grain size distributions can be used to tailor EBC microstructures to enhance the corrosion-resistance. Nevertheless, it should be noted that in order to conclude the most beneficial microstructural features for the EBC volatilization barrier, longer tests are required also under temperature gradients. Certainly, sintering of the porous Yb_2SiO_5 layer at the longer period of times and CTE mismatch stresses stemming from the higher CTE of the Yb_2SiO_5 layer, which will be more pronounced under thermal gradients, will likely affect the corrosion kinetics, as well. Another important outcome of this study is that a crystallization heat treatment of the amorphous as-deposited coating appears to be essential before the operation because crystalline coating revealed less severe corrosion degradation in comparison with the as-sprayed coating under the same testing conditions.

The authors acknowledge the contributions of IEK-1 members, Ralf Laufs for the APS experiments, Yoo Jung Sohn for XRD analyses and Christian Dellen for collecting the microscopy images.

[1] E.J. Opila, R.E. Hann, J. Am. Ceram. Soc. 80(1) (1997) 197-205.
[2] K.N. Lee, R.A. Miller, N.S. Jacobson, J. Am. Ceram. Soc. 78(3) (1995) 705-710.
[3] K.N. Lee, D.S. Fox, J.I. Eldridge, D. Zhu, R.C. Robinson, N.P. Bansal, R.A. Miller, J. Am. Ceram. Soc. 86(8) (2003) 1299-1306.
[4] K.N. Lee, D.S. Fox, N.P. Bansal, J. Eur. Ceram. Soc. 25(10) (2005) 1705-1715.
[5] E. Bakan, D. Marcano, D. Zhou, Y.J. Sohn, G. Mauer, R. Vaßen, J. Therm. Spray Technol. 26(6) (2017) 1011-1024.
[6] E. Bakan, G. Mauer, Y. Sohn, D. Koch, R. Vaßen, Coatings 7(4) (2017) 55.
[7] B.T. Richards, K.A. Young, F. de Francqueville, S. Sehr, M.R. Begley, H.N.G. Wadley, Acta Mater. 106 (2016) 1-14.
[8] E. Bakan, Y.J. Sohn, W. Kunz, H. Klemm, R. Vaßen, J. Eur. Ceram. Soc. 39(4) (2019) 1507-1513.
[9] R.C. Robinson, J.L. Smialek, J. Am. Ceram. Soc. 82(7) (1999) 1817-1825.
[10] M. Fritsch, PhD Thesis, Fakultät Maschinenwesen, Technische Universität Dresden, Germany, 2007.